ELSEVIER

International Journal of Mass Spectrometry 195/196 (2000) 625–638

International Journal of Mass Spectrometry

Gas-phase association reactions of hydroxide, methoxide, ethoxide, and their deuterated analogs

Shuji Kato, Thuy Thanh Dang[1], Stephan E. Barlow[2], Charles H. DePuy, Veronica M. Bierbaum*

Department of Chemistry and Biochemistry, University of Colorado, Boulder, CO 80309, USA

Received 3 August 1999; accepted 7 September 1999

Abstract

The selected ion flow tube technique is used to study 14 termolecular association reactions of hydroxide–water (OH^- + H_2O and OD^- + D_2O), methoxide–water (CH_3O^- + H_2O, CH_3O^- + D_2O, CD_3O^- + H_2O, and CD_3O^- + D_2O), methoxide–methanol (CH_3O^- + CH_3OH, CH_3O^- + CH_3OD, CD_3O^- + CD_3OH, and CD_3O^- + CD_3OD), and ethoxide–ethanol ($CH_3CH_2O^-$ + CH_3CH_2OH, $CH_3CD_2O^-$ + CH_3CD_2OH, $CD_3CH_2O^-$ + CD_3CH_2OH, and $CD_3CD_2O^-$ + CD_3CD_2OD) where the cluster bond dissociation energies are similar (~24–30 kcal/mol). The apparent second-order rate coefficients for association ($k_{II\ app}$) are measured as a function of helium pressure over the range of 0.25–1.2 Torr at 300 K. The derived termolecular rate coefficients and complex lifetimes are generally larger for systems with more degrees of freedom in the intermediate ion–molecule complex. In all reactions with alkoxides, association rates are significantly enhanced by deuteration of the alkyl groups (by factors of 1.4–3.0) whereas deuteration of the bridging hydrogen does not affect the association rates. Potential energy surfaces for association (single versus double well) are discussed based on the pressure dependence of the association rates. (Int J Mass Spectrom 195/196 (2000) 625–638) © 2000 Elsevier Science B.V.

Keywords: SIFT; Ion-association reactions; Hydroxide and alkoxide; Deuterium isotope effects; Double-well potential model

1. Introduction

In recent years there has been a growing interest in cluster ion chemistry, particularly with the view of using cluster systems as models for understanding condensed phase chemistry. One area of interest is to improve the understanding of the solvation process by examining the gas-phase association reactions of an ion with a neutral molecule [1,2]. Such processes are also relevant to molecular synthesis in interstellar clouds and planetary atmospheres [3]. Observation of hydrogen–deuterium (H/D) isotope effects gives clues to the mechanism and dynamics of association, both collisional and radiative. Although there have been a number of studies of the thermodynamics of cluster ions [1,2], there are relatively few studies on the effects of isotopic substitution on association kinetics. Adams and Smith [4] and Smith et al. [5] were the first to examine the kinetic isotope effects for

* Corresponding author.

[1] Present address: Department of Chemistry, Contra Costa College, 2600 Mission Bell Drive, San Pablo, CA 94806.

[2] Present address: Pacific Northwest National Laboratory, Richland, WA 99532.

Dedicated to Bob Squires, beloved friend and colleague.

PII S1387-3806(99)00197-9

the association reactions of CH_3^+ and its deuterated analogs with a number of neutrals including H_2, HD, and D_2. Association reactions of CH_3^+/CD_3^+ with HCN [6] and of Na^+ with NH_3 and ND_3 [7] have also been reported. All these studies show that deuterium substitution on methyl or ammonia increases the termolecular association rate coefficient by a factor of ~2 or more. This is interpreted by invoking an idea that the deuterated ion–molecule association complexes have longer unimolecular lifetimes and thus are subject to more collisional stabilization with the third body. More recently, Thölmann et al. [8] used Fourier transform ion cyclotron resonance (FTICR) spectrometry to systematically examine the H/D isotope effects on the low-pressure association reactions of protonated acetone with acetone $(CH_3)_2COH^+ + (CH_3)_2CO$. A striking result is that the unimolecular dissociation of the ion–molecule complex is slowed down by a factor of ~3 by deuteration of the methyl group, whereas deuteration on the bridging hydrogen does not affect the unimolecular lifetime. Radiative stabilization, on the other hand, was found to depend only on the isotope labeling of the bridging hydrogen [8].

To increase our understanding of isotope effects on the kinetics of association reactions, we have systematically investigated 14 termolecular association reactions of hydroxide–water, methoxide–water, methoxide–methanol, and ethoxide–ethanol and their deuterated analogs:

$$OH^- + H_2O \xrightarrow{He} HO^- \cdot H_2O \quad (1)$$

$$OD^- + D_2O \xrightarrow{He} DO^- \cdot D_2O \quad (2)$$

$$CH_3O^- + H_2O \xrightarrow{He} CH_3O^- \cdot H_2O \quad (3)$$

$$CH_3O^- + D_2O \xrightarrow{He} CH_3O^- \cdot D_2O \quad (4)$$

$$CD_3O^- + H_2O \xrightarrow{He} CD_3O^- \cdot H_2O \quad (5)$$

$$CD_3O^- + D_2O \xrightarrow{He} CD_3O^- \cdot D_2O \quad (6)$$

$$CH_3O^- + CH_3OH \xrightarrow{He} CH_3O^- \cdot HOCH_3 \quad (7)$$

$$CH_3O^- + CH_3OD \xrightarrow{He} CH_3O^- \cdot DOCH_3 \quad (8)$$

$$CD_3O^- + CD_3OH \xrightarrow{He} CD_3O^- \cdot HOCD_3 \quad (9)$$

$$CD_3O^- + CD_3OD \xrightarrow{He} CD_3O^- \cdot DOCD_3 \quad (10)$$

$$CH_3CH_2O^- + CH_3CH_2OH \xrightarrow{He} CH_3CH_2O^- \cdot HOCH_2CH_3 \quad (11)$$

$$CH_3CD_2O^- + CH_3CD_2OH \xrightarrow{He} CH_3CD_2O^- \cdot HOCD_2CH_3 \quad (12)$$

$$CD_3CH_2O^- + CD_3CH_2OH \xrightarrow{He} CD_3CH_2O^- \cdot HOCH_2CD_3 \quad (13)$$

$$CD_3CD_2O^- + CD_3CD_2OD \xrightarrow{He} CD_3CD_2O^- \cdot DOCD_2CD_3 \quad (14)$$

These particular choices are dictated by the following considerations: 1. each of these reactions can produce only a single product, and 2. the dissociation energies for these hydrogen-bonded clusters are very similar, ~24–30 kcal/mol; $HO^- \cdot H_2O$ (26.8 kcal/mol [9], 27.6 kcal/mol [10]), $DO^- \cdot D_2O$ (26.8 kcal/mol [9,11]), $CH_3O^- \cdot H_2O$ (23.9 kcal/mol [9,11]), $CH_3O^- \cdot HOCH_3$ (28.8 kcal/mol [9,11], 29.3 kcal/mol [10], 29.5 kcal/mol [12]), $CH_3O^- \cdot DOCH_3$ (28.3 kcal/mol [13]), $CD_3O^- \cdot HOCD_3$ (28.9 kcal/mol [13]), $CD_3O^- \cdot DOCD_3$ (28.5 kcal/mol [13]), and $CH_3CH_3O^- \cdot HOCH_2CH_3$ (27.6 kcal/mol [11], 28.3 kcal/mol [12]). We used the tandem flowing afterglow-selected ion flow tube (FA-SIFT) apparatus to measure the termolecular rates with helium. Of the 14 measurements, only the collisional association rates for hydroxide–water [Eq. (1)] [14] and methoxide–methanol [Eq. (7)] [12] have been previously reported. Early ICR measurements of Caldwell and Bartmess [15] showed that bimolecular, radiative association rates for methoxide-methanol [Eq. (7)] and ethoxide-ethanol [Eq. (11)] are immeasurably slow ($<5 \times 10^{-12}$ cm^3 molecule^{-1} s^{-1}), consistent with generalized theoretical work by Dunbar [16,17].

Proton transfer and association reactions of methoxide with methanol have attracted considerable interest, both experimentally and theoretically. The measured deuterium fractionation factor for the proton-bound dimer of methoxide and methanol (Weil and Dixon [18] and Wilkinson et al. [12]) revealed only a very low barrier for the intracluster proton transfer (~2 kcal/mol), consistent with the results of quantum chemical calculations [18–20]. This barrier is significantly smaller than the hydrogen-bonding stabilization energy for the cluster itself (≈29 kcal/mol), rendering the motion of a proton nearly free. Nevertheless, the proton transfer efficiency for the thermoneutral systems is found to be considerably less than the statistical value of 50% (Barlow et al. ≈0.35 [13]; Dodd et al. ≈0.26 [21]). This observation led to the idea that the methoxide–methanol system actually has a tight transition state inside of the loose orbiting transition state; fast unimolecular back dissociation of the initial loose complex hampers the methoxide–methanol pair from efficiently entering the tight, hydrogen-bonded complex where the proton transfer can take place. A high-pressure-limit association rate coefficient significantly less than the methoxide–methanol collision rate [12] is consistent with this system being a double well. The methoxide–methanol system has also been investigated through several different approaches. Baer and Brauman [22] employed infrared multiphoton dissociation (IRMPD) to dissociate isotopically labeled methoxide–methanol clusters derived from the Riveros reaction [23]. The product isotope abundance indicated that the cluster from this reaction is *not* the tight, hydrogen-bonded structure, suggestive of the existence of a second, loosely bound structure as mentioned above. Electron photodetachment spectroscopy of the same cluster showed that this complex has a smaller binding energy (≈19 kcal/mol) than the most stable, hydrogen-bonded cluster [24]. This second stable isomer, however, has eluded structural identification via quantum chemical calculations [12].

Significantly different theoretical approaches have also been made to explain the anomalous proton-transfer behavior of the methoxide-methanol system. Lim and Brauman [25] treated methoxide–methanol as a simple $[X \cdots H - X]^-$ system ($X = CH_3O$) with four internal degrees of freedom and they conducted trajectory calculations on a *barrierless* potential energy surface. They concluded that many trajectories, which have surmounted the usual (orbital angular momentum) centrifugal barrier, fail to enter into the deep, hydrogen-bonding well because of a "rotational locking" mechanism. This mechanism can account for the inefficient proton transfer and association reactions observed for methoxide-methanol, without assuming a second potential-energy minimum for the loose complex. This dynamic, *nonenergetic* transition state was later found to fulfill the criterion for a variational transition state [26]. Hinde and Ezra [27] did similar trajectory calculations specifically for the collinear approach of $CH_3O^- \rightarrow HOCH_3$, demonstrating that a certain fraction of trajectories "directly" exits the deep hydrogen-bonding well without forming a long-lived complex nor transferring the proton.

The origin of the "double well" (or "double transition state") behavior has thus been an issue of controversy. The ethoxide–ethanol reactions are of similar interest in this respect; experimental data strongly suggest that these reactions are also double-well systems. The proton-transfer efficiency (≈0.30) is significantly lower than 50% [21] despite the fact that the potential for the intracluster motion of the bridging hydrogen has only a small or no central maximum [28]. IRMPD experiments demonstrated once again that the ethoxide–ethanol cluster from the Riveros reaction is different from the most stable hydrogen-bonded structure [22]. On the other hand, hydroxide–water reactions have proton-transfer efficiencies that are near the statistical limit [14,21,29], suggesting that this system has a single well without any inner transition states. The methoxide–water reactions represent an interesting and possibly intermediate case between the hydroxide–water and methoxide–methanol systems. We systematically examine these 14 reactions with the aim of increasing our knowledge regarding the mechanism of ion–molecule association. Kinetic schemes for double-well systems will also be discussed in some detail.

2. Experimental

The experiments were carried out using the FA-SIFT which has been described previously in detail [30]. Hydroxide ion is produced by dissociative electron attachment with N_2O (forming O^-) followed by rapid hydrogen atom abstraction from methane. The OD^- ion is generated by reacting the OH^- ion with D_2O. Alkoxide ions (CH_3O^-, CD_3O^-, $CH_3CH_2O^-$, $CD_3CH_2O^-$, $CH_3CD_2O^-$, $CD_3CD_2O^-$) are produced by reacting OH^- with the appropriate alcohol. For example, $CD_3CH_2O^-$ is generated from the reaction of OH^- with CD_3CH_2OH. Once the desired reactant ion is produced, it is mass selected by the quadrupole mass filter and injected through a venturi inlet into the second flow tube. Known flows of reactant neutrals are then added and the association products are detected with a second quadrupole mass filter equipped with an electron multiplier.

Reaction rate coefficients were measured, for a given helium pressure, by monitoring the decrease of the reactant ion signal as a function of reaction distance using a constant flow rate of the neutral reagent. The reported rate coefficients are the averages of at least three independent measurements which are made with different neutral flow rates. This insured that stabilization of the ion-molecule complex was dominated by collisions with helium buffer under the experimental conditions. The standard deviation of a set of rate coefficient measurements was typically 15% or less, whereas we estimate the absolute accuracy of the rate coefficients to be $\pm 25\%$.

The experiments were performed at room temperature (300 K). Reagent purities were: D_2O (99.9 atom % D), CH_3OH (99.9%), CH_3OD (99.5%), CD_3OH (99.0%), CD_3OD (99.8%), CH_3CH_2OH (anhydrous), CH_3CH_2OD (99.5%), CH_3CD_2OH (98.0%), CD_3CH_2OH (98.0%), and CD_3CD_2OD (99.0%). Freeze–pump–thaw cycles were used to degas the liquid samples. The helium buffer gas (99.995%) was purified by passing it through a molecular sieve trap immersed in liquid nitrogen.

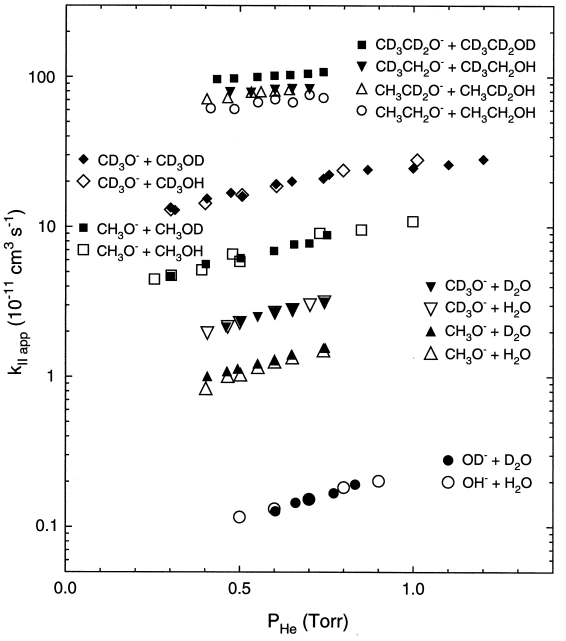

Fig. 1. Apparent bimolecular rate coefficients for association vs. helium pressure.

3. Results and discussion

3.1. Overview

Fig. 1 gives a summary of all the cluster systems studied. The apparent bimolecular rate coefficients for association (k_{IIapp}) are plotted versus helium pressure. The k_{IIapp} rate coefficient generally increases with the size of the cluster ions (or the increase in complexity), i.e. increasing in the order of hydroxide–water, methoxide–water, methoxide–methanol, and ethoxide–ethanol.

A comparison of the k_{IIapp} rate coefficients reveals distinctively different isotope effects. First, the rates for reaction pairs (1) and (2), (3) and (4), (5) and (6), (7) and (8), and (9) and (10) are identical within experimental uncertainty. This implies that the presence of either hydrogen or deuterium in the bridging position (i.e., the bonding position between the ion and neutral) does not affect the association rate; for example, $CH_3O^- \cdot HOCH_3$ versus $CH_3O^- \cdot DOCH_3$. Second, the k_{IIapp} values for reaction pairs (3) and (5),

Table 1
Rate coefficients and unimolecular lifetimes of the complex[a]

Reactants	k_f [b] (10^{-9} cm^3 s^{-1})	k_c [c] (10^{-10} cm^3 s^{-1})	$\frac{k_{\mathrm{IIapp,HP}}}{k_f}$ [d]	$k_{3,\mathrm{LP}}$ [d] (cm^6 s^{-1})	τ [e] (s^{-1})
$OH^- + H_2O$	3.02	5.60	. . .[f]	6.9×10^{-29} [f]	2.8×10^{-10} [f]
$OD^- + D_2O$	2.90	5.57			
$CH_3O^- + H_2O$	2.65	5.51	0.032	7.8×10^{-28} [g]	3.6×10^{-9} [g]
$CH_3O^- + D_2O$	2.56	5.51			
$CD_3O^- + H_2O$	2.61	5.50	0.062	1.6×10^{-27} [h]	7.4×10^{-9} [h]
$CD_3O^- + D_2O$	2.52	5.49			
$CH_3O^- + CH_3OH$	2.32	5.47	0.54	2.9×10^{-27}	1.5×10^{-8}
$CH_3O^- + CH_3OD$	2.31	5.46			
$CD_3O^- + CD_3OH$	2.22	5.45	0.53	8.2×10^{-27}	4.5×10^{-8}
$CD_3O^- + CD_3OD$	2.21	5.45			
$CH_3CH_2O^- + CH_3CH_2OH$	2.07	5.42	0.91	3.1×10^{-26}	1.8×10^{-7}
$CH_3CD_2O^- + CH_3CD_2OH$	2.03	5.41	0.91	4.1×10^{-26}	2.5×10^{-7}
$CD_3CH_2O^- + CD_3CH_2OH$	2.01	5.41			
$CD_3CD_2O^- + CD_3CD_2OD$	1.96	5.40	0.92	5.7×10^{-26}	3.6×10^{-7}

[a] At 300 K: τ, $k_{\mathrm{IIapp,HP}}/k_f$ and $k_{3,\mathrm{LP}}$ are calculated for sets of two reactions, as shown where applicable.
[b] Parameterized trajectory collision rate [31] for the reactants.
[c] Langevin collision rate [32] for collision of the association complex with helium.
[d] Calculated using the double-well model.
[e] Unimolecular lifetime of the complex [β(He) ≡ 0.15].
[f] Calculated using the single-well model.
[g] Values with the single-well model (including radiative stabilization) are 5.8×10^{-28} and 2.7×10^{-9}, respectively (see text).
[h] Values with the single-well model (including radiative stabilization) are 1.1×10^{-27} and 5.4×10^{-9}, respectively (see text).

(4) and (6), (7) and (9), and (8) and (10) are very different. This difference indicates that substitution of deuterium for hydrogen in the alkyl groups causes a large increase in the association rate; for example, $CD_3O^- \cdot HOCD_3$ versus $CH_3O^- \cdot HOCH_3$. Within the deuterated ethoxide–ethanol systems it appears that the association rate generally increases with the number of deuterium atoms in the alkyl groups, although the k_{IIapp} values for the reaction pair (12) and (13) are essentially identical within experimental uncertainty.

We analyze the apparent rate coefficients to extract the low-pressure-limit termolecular association rate coefficient ($k_{3,\mathrm{LP}}$), and use it to deduce the unimolecular lifetime of the complex (τ) as will be described. Reaction pairs with identical values of k_{IIapp} are analyzed as grouped. Results are summarized in Table 1. The fitting error depends strongly on the reaction and the model used, but the trend in fit values of $k_{3,\mathrm{LP}}$ is found to be entirely consistent with that observed for k_{IIapp}. We focus on this systematic trend, rather than the absolute values, in the following discussions.

3.2. Hydroxide–water

This system may be analyzed using a barrierless, single-well scheme for association [Eqs. (15)–(17)]. In general, the association of an anion (A^-) and neutral (B) can involve termolecular [Eq. (16)] and/or radiative [Eq. (17)] stabilization processes:

$$A^- + B \underset{k_b}{\overset{k_f}{\rightleftharpoons}} (A^- \cdot B)^* \quad (15)$$

$$(A^- \cdot B)^* + M \overset{\beta k_c}{\rightarrow} AB^- \quad (16)$$

$$(A^- \cdot B)^* \overset{k_r}{\rightarrow} AB^- + h\nu \quad (17)$$

where k_f is the rate coefficient for collision of A^- and B and k_b is that for unimolecular dissociation of the intermediate complex $(A^- \cdot B)^*$. The energetic com-

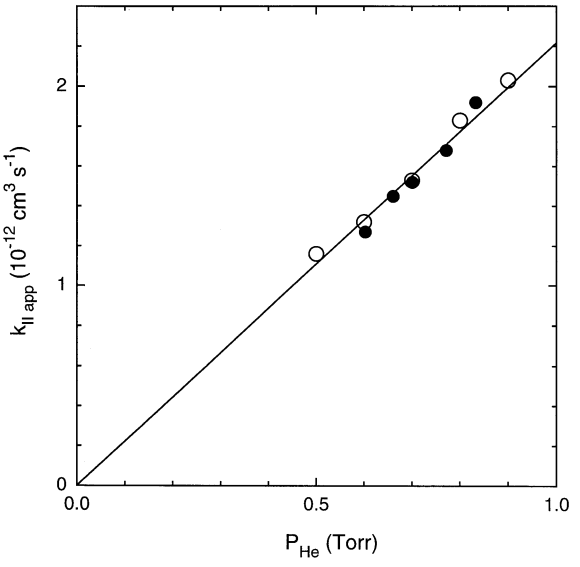

Fig. 2. Apparent bimolecular rate coefficients for $OH^- + H_2O$ (open circle) and $OD^- + D_2O$ (closed circle) plotted against helium pressure. Line is the best fit using the single-well model.

plex is deactivated to the stable cluster AB^- by collision with a third body M (=He) (the rate coefficient βk_c where β is the stabilization efficiency for helium) and/or by photon emission (the rate coefficient k_r). We compute the values of k_f and k_c using the parameterized trajectory [31] and Langevin [32] collision theories, respectively (Table 1). The trajectory theory appears to work well for the present systems; e.g. the calculated value of k_f for $CH_3O^- + CH_3OH$ (2.32×10^{-9} cm^3 molecule^{-1} s^{-1}) is in excellent agreement with that deduced from rapid ion–molecule reactions involving CH_3OH of $2.3 \pm 0.2 \times 10^{-9}$ cm^3 molecule^{-1} s^{-1} [13]. Milligan et al. have shown that the collisional stabilization efficiencies with helium buffer can be significantly smaller than those with the parent gas [33], the *relative* efficiency being 0.15 for the deactivation of protonated acrylonitrile dimer. The *absolute* values of β(He) are generally not known. We thus assume β(He) to be 0.15 throughout the present study. This approximation does not affect the qualitative discussion in this paper.

Fig. 2 plots k_{IIapp} versus helium pressure (P_{He}) for $OH^- + H_2O$ and $OD^- + D_2O$ association reactions. The plot appears to extrapolate to zero as $P_{\mathrm{He}} \rightarrow 0$, indicating that the bimolecular radiative process [Eq. (17)] is negligibly slow for this system (a separate analysis including the radiative association reveals little evidence for this process, with the zero-pressure intercept in Fig. 2 of the order of 10^{-14} cm^3 molecule^{-1} s^{-1} or less). With the steady-state approximation applied to $(A^- \cdot B)^*$ in Eqs. (15) and (16), $k_{\mathrm{IIapp}} = k_f\beta k_c[\mathrm{M}]/(k_b + \beta k_c[\mathrm{M}])$ or alternatively,

$$\frac{1}{k_{\mathrm{IIapp}}} = \frac{1}{k_f} + \frac{(k_b/\beta)}{k_f k_c} \cdot \frac{1}{[\mathrm{M}]} \tag{18}$$

where k_b/β is the fitting parameter in the plot of $1/k_{\mathrm{IIapp}}$ versus 1/[M]. The solid line in Fig. 2 is the result from the best fit of Eq. (18) to the experimental data. The low-pressure-limit termolecular association rate coefficient ($k_{3,\mathrm{LP}}$) is obtained from the slope in Eq. (18) as

$$k_{3,\mathrm{LP}} = \frac{\beta k_f k_c}{k_b} \tag{19}$$

The complex unimolecular lifetime (τ), which equals $1/k_b$, is derived using the assumed value of β(He). The obtained rate coefficients and fit values are summarized in Table 1.

The appropriateness of the barrierless single-well model for this system is supported by the efficient proton transfer reactions of $OH^- + D_2O$ [21,29] and $OD^- + H_2O$ [14,29]. After correcting for the reaction degeneracies and enthalpies [21] (the experimental efficiencies in [14] and [29] must also be corrected using the parameterized trajectory rates, as pointed out in [21]), the observed efficiencies are found to be fairly close to the maximum values calculated for the long-lifetime limits, where all the H and D atoms can scramble.

3.3. Alkoxide–alcohol

The analytical scheme using Eqs. (15) and (16) cannot fit the methoxide–methanol data. The discrepancy is twofold. First, nonzero intercepts are observed in the plots of k_{IIapp} versus helium pressure. Second, the high-pressure limit apparent bimolecular rate co-

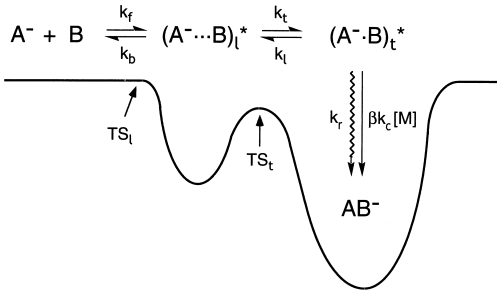

Fig. 3. Schematic potential energy surface for the double-well model with an "energetic" transition state (TS_t) located between the loose and tight complexes. The loose, orbiting transition state is denoted by TS_l.

efficient for association ($k_{\mathrm{IIapp,HP}}$) has been observed to be significantly less than the collision rate [12], whereas the single-well scheme above [Eq. (18)] predicts that it will equal k_f. A simple model that can account for the experimental results is a double-well model (Fig. 3)

$$A^- + B \underset{k_b}{\overset{k_f}{\rightleftharpoons}} (A^- \cdots B)_l^* \tag{20}$$

$$(A^- \cdots B)_l^* \underset{k_l}{\overset{k_t}{\rightleftharpoons}} (A^- \cdot B)_t^* \tag{21}$$

$$(A^- \cdot B)_t^* + M \overset{\beta k_c}{\rightarrow} AB^- \tag{22}$$

$$(A^- \cdot B)_t^* \overset{k_r}{\rightarrow} AB^- + h\nu \tag{23}$$

In this scheme, a loosely bound complex $(A^- \cdots B)_l^*$ is in equilibrium with the reactant and with a hydrogen-bonded, more tightly bound complex $(A^- \cdot B)_t^*$. The tight complex then is stabilized by collisional deactivation and/or photon emission; the loose complex does not live long enough for these stabilization processes to be effective. In theory the tight complex can also be in direct equilibrium with the reactant, but the complex can be approximated to be isolated from the reactant for the present systems (see the Appendix).

The double-well model using Eqs. (20)–(23) has been discussed elsewhere by Meot-Ner [34], and we examine it in further detail here. Applying a steady-state approximation to both the loose and tight complexes, we obtain an expression for k_{IIapp} as

$$\frac{1}{k_{\mathrm{IIapp}}} = \frac{1 + (k_b/k_t)}{k_f} + \frac{(k_b/k_t)(k_l/\beta)}{k_c[\mathrm{M}] + (k_r/\beta)} \cdot \frac{1}{k_f} \tag{24}$$

Fitting k_{IIapp} to [M] using Eq. (24) returns three sets of parameters k_b/k_t, k_l/β, and k_r/β. The high-pressure-limit $k_{\mathrm{IIapp,HP}}$ is now $k_f/(1 + k_b/k_t)$, which is smaller than k_f by the factor of $(1 + k_b/k_t)$. Eq. (24) is expanded in a series of 1/[M], and for a high-pressure limit where $k_r \ll \beta k_c[\mathrm{M}]$,

$$\frac{1}{k_{\mathrm{IIapp}}} \approx \frac{1 + (k_b/k_t)}{k_f} + \frac{(k_b/k_t)(k_l/\beta)}{k_f k_c} \cdot \frac{1}{[\mathrm{M}]} - \frac{(k_b/k_t)(k_l/\beta)(k_r/\beta)}{k_f k_c^2} \cdot \frac{1}{[\mathrm{M}]^2} \tag{25}$$

The second term in Eq. (25) ensures that $k_{3,\mathrm{LP}}$ is obtained from the initial slope, i.e. the *high-pressure* asymptotic slope, of the $1/k_{\mathrm{IIapp}}$ versus 1/[M] plot.

$$k_{3,\mathrm{LP}} = \frac{k_f k_c}{(k_b/k_t)(k_l/\beta)} = \frac{\beta k_f k_c}{(k_l/k_t)k_b} \tag{26}$$

By comparing Eqs. (19) and (26), we can deduce that the denominator in Eq. (26), $(k_l/k_t)k_b$, is in fact the effective unimolecular dissociation rate ($k_{b,\mathrm{eff}}$) of the tight complex, i.e. the most stable form of the complex. The unimolecular lifetime of the association complex is thus given by $\tau_{\mathrm{eff}} = 1/k_{b,\mathrm{eff}}$. In contrast to Eq. (18), a plot of $1/k_{\mathrm{IIapp}}$ versus 1/[M] is no longer linear for Eq. (25) and the deviation from linearity (the third term) corresponds to the radiative process.

Fig. 4 shows the $1/k_{\mathrm{IIapp}}$ versus 1/[M] plots for the methoxide–methanol systems, with the alkyl groups deuterated [Eqs. (9) and (10)] and undeuterated [Eqs. (7) and (8)]. A deviation from linearity may be observed in the low [M] region for both plots, and the data are nicely fit with the solid lines using Eq. (24). The fit value of $k_{\mathrm{IIapp,HP}}$ for CH_3O^- + CH_3OH (and for CH_3O^- + CH_3OD) is $\approx 1.3 \times 10^{-9}$ cm^3 $molecule^{-1}$ s^{-1}, which is about half the collision rate k_f (Table 1). This is in excellent agreement with the $k_{\mathrm{IIapp,HP}}$ value from the direct high-pressure-mass spectrometry (HPMS) measurement of Wilkinson et

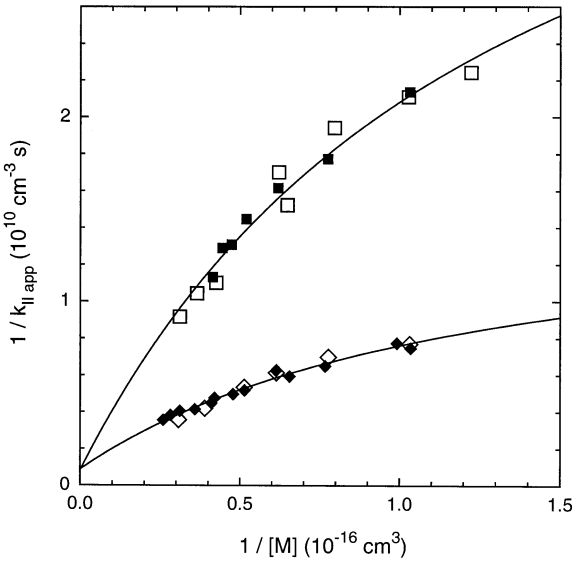

Fig. 4. Plots of $1/k_{\mathrm{IIapp}}$ vs. 1/[M] (M = helium) for CH_3O^- + CH_3OH (open square), CH_3O^- + CH_3OD (closed square), CD_3O^- + CD_3OH (open diamond), and CD_3O^- + CD_3OD (closed diamond). Lines are the best fits using the double-well model (with the radiative association term included).

al. [12], extrapolated to 300 K. The termolecular association rate coefficients and lifetimes (τ_{eff}) for the methoxide–methanol systems, on average, are two orders of magnitude larger than that for hydroxide–water. The lifetime for the alkyl-deuterated reactants is significantly larger than that for nondeuterated reactants.

At the low pressure limit, the k_{IIapp} for CH_3O^- + CH_3OH (and for CH_3O^- + CH_3OD) extrapolates to $\approx 2 \times 10^{-11}$ cm^3 $molecule^{-1}$ s^{-1}, which exceeds the upper limit for the radiative stabilization of 5×10^{-12} that was estimated from the ICR measurements by Caldwell and Bartmess [15]. A separate analysis omitting the radiative term k_r in Eq. (24) yields a less satisfactory, straight line fit that returns an anomalously small value of $k_{\mathrm{IIapp,HP}}$ ($\approx 1.7 \times 10^{-10}$); only $\approx$7% of the collision rate. Thus radiative stabilization is likely to be responsible for the curvature observed in the lower pressure region of Fig. 4 but the radiative rate extrapolated using Eq. (24) is somehow an overestimation. We believe that this discrepancy may be explained by the fact that the back-dissociation rate k_b is actually pressure dependent and can differ significantly between experimental conditions for SIFT ($\approx 10^{-1}$ Torr) and ICR (10^{-8}–10^{-6} Torr). At high pressures, only more energetic complexes with shorter lifetimes can avert collisional deactivation and back-dissociate to the reactants. As a result, the apparent k_b may increase by several orders of magnitude in going from the ICR to SIFT (or HPMS) measurements. The change in apparent k_b causes a substantial underestimation (by several orders of magnitude) of the *high-pressure-limit* bimolecular rate coefficient $k_{\mathrm{IIapp,HP}}$ when extrapolated from the *low-pressure* measurements using ICR. The effect of changing k_b on $k_{\mathrm{IIapp,HP}}$ is discussed in a detailed review of Meot-Ner [34]. The situation with the radiative rate can be the opposite. When k_b is changing significantly, the radiative rate can be more accurately derived by using k_b from *low-pressure* measurements or ultimately by directly measuring the bimolecular rate near zero pressure. Henceforth we will take the derived rates for radiative stabilization only as qualitative guidelines.

The value of $k_{3,\mathrm{LP}}$ is found to be relatively insensitive to the magnitude of the unknown radiative rate; as discussed above, this value is derived from the high-pressure asymptotic slope. Analysis omitting the radiative term (i.e. $k_r \equiv 0$) systematically increases the values of $k_{3,\mathrm{LP}}$ (and τ), but by only a factor of 2 for the methoxide–methanol system. This deviation, however, prevents quantitative conclusions. Therefore, we will focus on the qualitative trends of $k_{3,\mathrm{LP}}$, complex lifetime, and the associated fitting parameters in the following discussion.

Ethoxide–ethanol reactions are analyzed using the same model as above; a single-well model with Eqs. (15) and (16) cannot adequately fit the data whereas other studies strongly suggest a double-well scheme [21,22]. Because of the limited pressure range that can be studied (Fig. 1), the data can be fit either with or without the radiative term in Eq. (24). Nevertheless, omission of the radiative term yields larger values of $k_{3,\mathrm{LP}}$ by a factor of about 4. This difference, however, does not alter the qualitative discussion; the derived values of $k_{3,\mathrm{LP}}$ and τ_{eff} are one order of magnitude larger for ethoxide-ethanol systems than for methox-

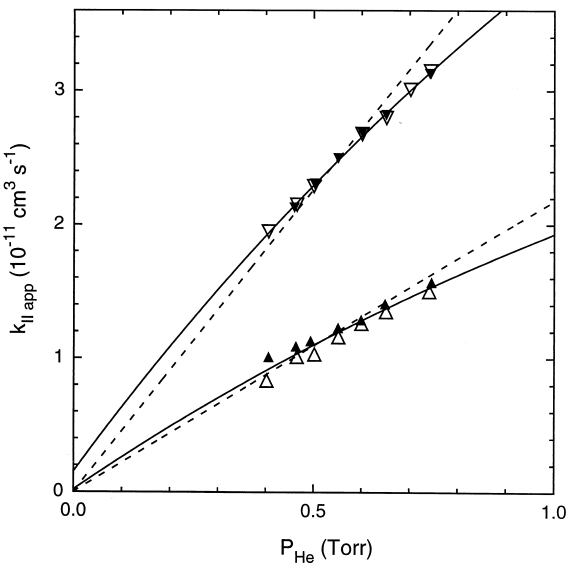

Fig. 5. Apparent bimolecular rate coefficients for CH_3O^- + H_2O (open triangle), CH_3O^- + D_2O (closed triangle), CD_3O^- + H_2O (open inverted triangle), and CD_3O^- + D_2O (closed inverted triangle) plotted against helium pressure. Solid lines are the best fits using the double-well model (with the radiative association term included). Broken lines are the best fits using the single-well model without radiative association.

ide-methanol systems. These values are found to increase with progressive deuteration of the ethyl groups (Table 1).

3.4. Methoxide–water

Fig. 5 plots k_{IIapp} versus helium pressure for the methoxide–water reactions with the methyl groups deuterated [Eqs. (3) and (4)] and undeuterated [Eqs. (5) and (6)]. This system may be an intermediate case between the hydroxide-water and methoxide-methanol systems. The single-well model using Eq. (18) does not fit the data perfectly; there are small but nonzero intercepts for k_{IIapp} which are more obvious for the alkyl-deuterated reactants. Inclusion of a radiative process in the single-well scheme significantly improves the fit (not shown in Fig. 5). For example CH_3O^- + H_2O (and CH_3O^- + D_2O) is fit with a zero-pressure intercept of $\approx 2 \times 10^{-12}$ cm^3 molecule^{-1} s^{-1}, which, along with the discussion above, may be marginally acceptable in view of an upper limit for a more complex but relevant system CH_3O^- + CH_3OH (5×10^{-12}) [15]. A double-well model with a radiative term [Eq. (24)] gives equally excellent fits, now with a possibly more reasonable intercept of $\approx 2 \times 10^{-13}$ cm^3 molecule^{-1} s^{-1} for CH_3O^- + H_2O (and CH_3O^- + D_2O).

In any event, the fitting alone cannot determine whether the potential energy surface for the methoxide–water association is single-well or double-well. The values of $k_{3,\mathrm{LP}}$ and complex lifetime are calculated based on the double-well model and are shown in Table 1. These values are found to be only marginally sensitive to the model assumption; the single-well/radiative scheme yields values that are only ≈20% smaller than from the double-well scheme. As expected, these values lie between those for hydroxide–water and alkoxide–alcohol, and once again the methyl–deuterated system has a longer lifetime.

3.5. Size and isotope effects in termolecular association

Fig. 6 is a plot of the cluster ion lifetimes (from Table 1) as a function of vibrational degrees of freedom of the cluster ions studied. The lifetimes have been deduced using the same value of β(He) for all reactions. Given similar internal energies due to the similar hydrogen-bonding stabilization (∼24–30 kcal/mol), a larger cluster would have a lower vibrational temperature and can thus suffer less efficient collisional stabilization. On the other hand, a larger cluster has more vibrational modes with lower frequencies that can facilitate more efficient vibration-to-translation energy loss with helium [35]. The assumption of constant β(He) might thus be justified to a first-order approximation. As apparent in Fig. 6, the lifetime increases with the size of the cluster ions. This trend is consistent with that observed for the raw k_{IIapp} plots (Fig. 1). The size effect is readily interpreted in terms of the Rice-Ramsperger-Kassel-Marcus (RRKM) theory [36]; the lifetime increases because the complexity of the clusters increases whereas their internal energies, i.e. the hydrogen-bonding stabilization, remain fairly similar. As Meot-Ner pointed

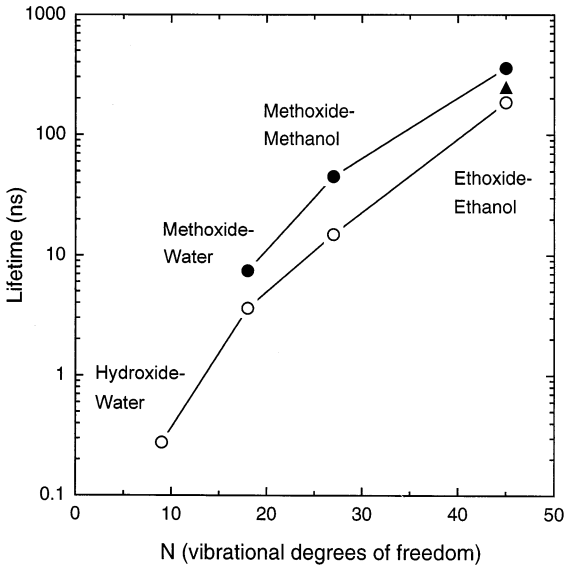

Fig. 6. Unimolecular lifetimes of the association complexes as a function of vibrational degrees of freedom (data from Table 1). Closed symbols for alkoxide systems are for reactants with the alkyl groups deuterated. The closed triangle is for ethoxide-ethanol with the alkyl groups partially deuterated.

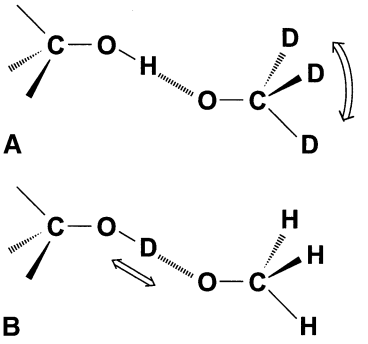

Fig. 7. Schematic vibrational modes for the hydrogen-bonded alkoxide-alcohol complex with deuterium substitution (A) on the alkyl group and (B) on the bridging hydrogen.

out [34], RRKM treatment alone is not sufficient when the potential surface involves a double well with a loose complex in which dynamic effects may come into play. Nevertheless, the present results suggest that this interpretation is qualitatively correct.

The lifetime increases with deuterium substitution of the alkyl group, by factors of 2.1 (methoxide–water), 3.0 (methoxide–methanol), and 2.0 (completely deuterated ethoxide–ethanol). The increase of the lifetime for the partially deuterated ethoxide–ethanols $CH_3CD_2O^- \cdot HOCD_2CH_3$ and $CD_3CH_2O^- \cdot HOCH_2CD_3$, with four and six deuterium atoms on the alkyl groups, respectively, is less spectacular ($\approx$1.4 on average) than that for $CD_3CD_2O^- \cdot DOCD_2CD_3$ with ten deuterium atoms on the alkyl groups (Fig. 6). The observed magnitudes of lifetime enhancement by deuterium substitution are similar to those observed previously for other cluster systems [4–8]. In the language of RRKM, the density of available states in the complex is considerably increased by deuterium substitution. These states must arise from the low frequency modes. Thus the lifetime increases must be dominated by the internal rotations which are only weakly hindered (Fig. 7). For the $CH_3O^- \cdot H(D)OCH_3$ cluster, the calculated five lowest frequencies ($<$200 cm^{-1}) are due to the methyl torsions and the torsion about the O–O axis [18]. The essentially identical lifetimes observed for $CH_3CD_2O^- \cdot HOCD_2CH_3$ and $CD_3CH_2O^- \cdot HOCH_2CD_3$ suggest that the internal rotation about the C–O axis, rather than the C–C axis, dominates the increase of the density of states for the ethoxide–ethanol clusters.

The isotope effect arises from conversion of the alkoxy groups from free to weakly hindered rotors upon passing through the orbiting transition state and entering the potential well for association. Actually, the microcanonical unimolecular lifetime is proportional to the density of states, $N^*(E^*)$, of the complex but is also *inversely* proportional to the sum of states, $\sum P(E^{\dagger}_{vr})$, of the orbiting transition state [35], both of which increase as a result of deuterium substitution. Kemper et al. [6], however, showed for similar isotopically labeled $CH_3^+/CD_3^+ + HCN$ association reactions that the increase of $N^*(E^*)$ prevails over the increase of $\sum P(E^{\dagger}_{vr})$, reproducing the overall lifetime increase of $\sim$2 that they observed experimentally. We believe that this argument also holds for our reactions.

Deuterium substitution on the bridging position, on the other hand, does not affect the cluster lifetime. The lack of isotope effect for the bridging position suggests that the high vibrational frequencies, O–H

and O–D (Fig. 7), do not substantially increase the density of states of the complex (e.g. ν(O–H–O) = 2124 cm^{-1} and ν(O–D–O) = 1497 cm^{-1} for the asymmetric stretching in methoxide–methanol [18]). A more recent frequency calculation (modes unassigned) is found in [12]). These site-specific, kinetic isotope effects have been observed for other ion–molecule clusters of protonated acetone with acetone [8].

3.6. Loose versus tight complexes

Within the framework of the double-well model [Eq. (26)], the rate coefficient $k_{b,\mathrm{eff}}$ for the back unimolecular dissociation of the hydrogen-bonded complex scales linearly with the product of two fitting parameters, k_b/k_t and k_l/β

$$k_{b,\mathrm{eff}} = \frac{\beta k_f k_c}{k_{3,\mathrm{LP}}} = \beta(k_b/k_t)(k_l/\beta) \quad (27)$$

The k_b/k_t component represents the competition between back dissociation versus isomerization of the loose complex whereas k_l/β represents the competition between back isomerization versus collisional stabilization of the tight complex. We examine the contribution of each component to the unimolecular lifetime of the complex. Fig. 8 illustrates the correlation between $k_f k_c/k_{3,\mathrm{LP}}$ ($=k_{b,\mathrm{eff}}/\beta$) and fitting parameters k_b/k_t and k_l/β for methoxide–water [Eqs. (3)–(6)], methoxide–methanol [Eqs. (7)–(10)], and ethoxide–ethanol [Eqs. (11)–(14)]. The methoxide–water systems are treated as double wells and are included in Fig. 8. Conservatively, two features are apparent; $k_f k_c/k_{3,\mathrm{LP}}$ correlates strongly with k_b/k_t whereas k_l/β appears nearly unchanged. This suggests that the back dissociation of the loose complex dominates the overall lifetime of the hydrogen-bonded cluster, consistent with the double-well scheme that involves a short-lived loose complex.

Recently, Wilkinson et al. conducted extensive and important studies on the thermodynamic and kinetic properties of the methoxide–methanol complex [12]. Their results are consistent with the double-well scheme for this system; they used HPMS to reveal

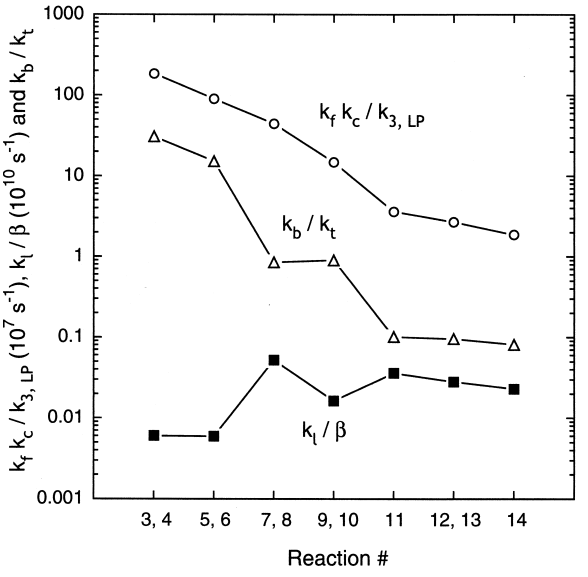

Fig. 8. Correlation between $k_f k_c/k_{3,\mathrm{LP}}$ ($=k_{b,\mathrm{eff}}/\beta$) and fit parameters for the double-well model (k_b/k_t and k_l/β) for reactions of methoxide–water [Eqs. (3)–(6)], methoxide–methanol [Eqs. (7)–(10)], and ethoxide–ethanol [Eqs. (11)–(14)].

that the $k_{\mathrm{IIapp,HP}}$ is significantly lower than the collision limit k_f. In addition, the observed decrease of the association rate coefficient with increasing temperature [12] suggested a double minimum potential energy surface; the transition state between the loose and tight complexes (TS_t in Fig. 3) is located slightly below the reactant energy. The measured entropy of activation for the complex unimolecular dissociation suggested that the TS_t is only marginally less constrained than the proton-bound complex itself [12]. With regard to the last point, a direct and precise HPMS determination of $k_{\mathrm{IIapp,HP}}$ (and hence k_b/k_t) for alkyl-deuterated methoxide–methanol [Eq. (9) or (10)] would be particularly interesting; if the TS_t structure is close to that of the tight complex, the isotope effect might have to originate earlier in the loose complex. Then the k_b/k_t term, rather than the k_l/β term, will reflect the isotope effect. Our values of k_b/k_t deduced indirectly from the model fitting (Fig. 8) are not precise enough to address this question.

The IRMPD [22] and electron photodetachment spectroscopy [24] of alkoxide-alcohol dimers from the Riveros reaction [23]

$$RO^- + HCOOR' \rightarrow [ROH \cdots COOR']^- \xrightarrow{-CO} ROH \cdot {}^-OR' \quad (28)$$

have demonstrated that the ion–molecule complexes from this reaction are different from the most stable hydrogen-bonded structure, suggesting the existence of a second stable structure for the alkoxide–alcohol association complex. However, the loose complex, presumably an S_N2-type structure with the alkoxy unit trapped behind the alkyl umbrella and shielded from the bridging hydrogen [12,22], has eluded quantum chemical identification. As shown above, our data on the *methoxide–water* reactions are not conclusive; the reactions can be analyzed using both single- and double-well models. It is very intriguing if this system is indeed a double well, because, in contrast to the alkoxide-alcohol systems, there appears to be no steric hindrance for the methoxide to approach one of the bridging hydrogens on water to form the most stable cluster. Alternatively, since the double-well-like behavior ($k_{\mathrm{IIapp,HP}} < k_f$) might also be explained in terms of rotational locking on a barrierless surface [25], trajectory calculations for the methoxide–water system would be insightful. However, it would also be required that the rotational locking mechanism account for the isotope effects observed. The value of $k_{\mathrm{IIapp,HP}}/k_f$ may be extremely sensitive to the assumed potential energy surface for this system; a single well would predict this term to be nearly unity whereas a double well would predict it to be significantly smaller ($\sim 10^{-2}$, Table 1). This enormous difference could be experimentally discernible even in the presence of a possible direct collision mechanism [27], although experimental approaches using, e.g. HPMS, might not be straightforward because of the extremely fast back unimolecular dissociation of methoxide–water.

4. Conclusions

Termolecular association reactions of hydroxide–water, methoxide–water, methoxide–methanol, ethoxide–ethanol, and their deuterated analogs were studied. The association rate coefficients and complex lifetimes are found to be generally larger for systems with more degrees of freedom in the intermediate complex, reflecting longer complex lifetimes for larger systems. Distinctly different isotope effects are observed. In all reactions with alkoxides, association rates are significantly enhanced by deuteration of the alkyl groups whereas deuteration of the bridging hydrogen does not affect the association rates. Within the deuterated ethoxide–ethanol systems, the lifetime is controlled by the number of deuterium atoms in the alkyl groups. The isotope effects suggest that the lifetime increases are dominated by the increase of the density of states provided by the low frequency modes, which are due to weakly hindered internal rotations of the alkoxy groups in the complex.

Measured pressure dependence of the association rate coefficients was discussed using a single- or double-well model for the potential energy surface for association. The association of hydroxide–water proceeds on a single well surface whereas those of methoxide–methanol and ethoxide–ethanol are best described as proceeding on a double-well surface, which accommodates an initial loose complex and a hydrogen-bonded tight complex. The association of methoxide-water can be interpreted using either model, and the experimental data do not allow us to distinguish the two. For systems with a double well surface, it is suggested that the back unimolecular dissociation of the loose complex dominates the overall complex lifetime.

Acknowledgement

The authors gratefully acknowledge support of this work by National Science Foundation grant nos. CHE-9421756 and CHE-9734867.

Appendix

A more general scheme involving a direct equilibrium between the tight complex and reactants is

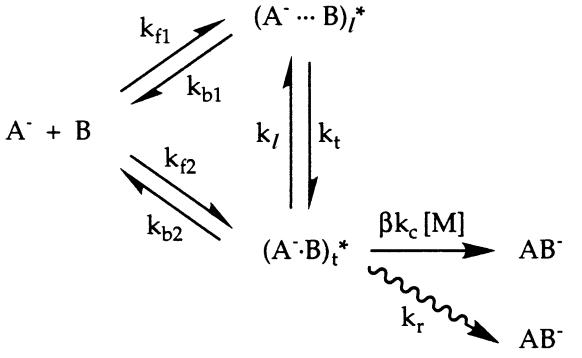

(29)

A steady-state approximation for the loose and tight complexes gives

$$\frac{1}{k_{\mathrm{IIapp}}} = \frac{1}{k_{f2} + k_{f1}/(1 + k_{b1}/k_t)} + \frac{k_{b2} + k_l/(1 + k_t/k_{b1})}{k_{f2} + k_{f1}/(1 + k_{b1}/k_t)} \cdot \frac{1}{\beta k_c[\mathrm{M}] + k_r} \tag{30}$$

When $k_r \ll \beta k_c[\mathrm{M}]$,

$$\frac{1}{\beta k_c[\mathrm{M}] + k_r} \approx \frac{1 - k_r/(\beta k_c[\mathrm{M}])}{\beta k_c[\mathrm{M}]} \tag{31}$$

And hence,

$$\frac{1}{k_{\mathrm{IIapp}}} \approx \frac{1}{k_{f2} + k_{f1}/(1 + k_{b1}/k_t)} + \gamma \cdot \frac{1}{[\mathrm{M}]} + \delta \cdot \frac{1}{[\mathrm{M}]^2} \tag{32}$$

The denominator of the first term, which is obtained when $[\mathrm{M}] \rightarrow \infty$ in the plot of $1/k_{\mathrm{IIapp}}$ versus 1/[M], is the high-pressure-limit bimolecular rate coefficient, $k_{\mathrm{IIapp,HP}}$. An experimental observation that the $k_{\mathrm{IIapp,HP}}$ for methoxide/methanol (300 K) is only about half the collision rate ($=k_{f2} + k_{f1}$) [12] requires that k_{f2} be insignificant with respect to k_{f1} and that k_{b1}/k_t be comparable to or greater than 1. Thus the direct formation of the tight complex is insignificant in this system and the kinetic scheme is reduced to Eqs. (20)–(23). Eq. (30) reduces to Eq. (24) by replacing k_{f2} (and hence k_{b2}) with zero and, accordingly, replacing k_{f1} and k_{b1} with k_f and k_b, respectively.

References

[1] P. Kebarle, Annu. Rev. Phys. Chem. 28 (1977) 445.
[2] R.G. Keesee, A.W. Castleman Jr., J. Phys. Chem. Ref. Data 15 (1986) 1011.
[3] V.G. Anicich, A.D. Sen, W.T. Huntress Jr., M.J. McEwan, J. Chem. Phys. 93 (1990) 7163.
[4] N.G. Adams, D. Smith, Chem. Phys. Lett. 79 (1981) 563.
[5] D. Smith, N.G. Adams, E. Alge, J. Chem. Phys. 77 (1982) 1261.
[6] P.R. Kemper, L.M. Bass, M.T. Bowers, J. Phys. Chem. 89 (1985) 1105.
[7] R. Passarella, A.W. Castleman Jr., J. Phys. Chem. 93 (1989) 5840.
[8] D. Thölmann, A. McCormick, T.B. McMahon, J. Phys. Chem. 98 (1994) 1156.
[9] M. Meot-Ner (Mautner), L.W. Sieck, J. Phys. Chem. 90 (1986) 6687.
[10] G.J.C. Paul, P. Kebarle, J. Phys. Chem. 94 (1990) 5184.
[11] M. Meot-Ner (Mautner), L.W. Sieck, J. Am. Chem. Soc. 108 (1986) 7525.
[12] F.E. Wilkinson, M. Peschke, J.E. Szulejko, T.B. McMahon, Int. J. Mass Spectrom. Ion Processes 175 (1998) 225.
[13] S.E. Barlow, T.T. Dang, V.M. Bierbaum, J. Am. Chem. Soc. 112 (1990) 6832.
[14] J.J. Grabowski, C.H. DePuy, J.M. Van Doren, V.M. Bierbaum, J. Am. Chem. Soc. 107 (1985) 7384.
[15] G. Caldwell, J.E. Bartmess, J. Phys. Chem. 85 (1981) 3571.
[16] R.C. Dunbar, Int. J. Mass Spectrom. Ion Processes 100 (1990) 423.
[17] R.C. Dunbar, Int. J. Mass Spectrom. Ion Processes 160 (1997) 1.
[18] D.A. Weil, D.A. Dixon, J. Am. Chem. Soc. 107 (1985) 6859.
[19] J.H. Busch, J.R. de la Vega, J. Am. Chem. Soc. 99 (1977) 2397.
[20] S. Wolfe, S. Hoz, C.-K. Kim, K. Yang, J. Am. Chem. Soc. 112 (1990) 4186.
[21] J.A. Dodd, S. Baer, C.R. Moylan, J.I. Brauman, J. Am. Chem. Soc. 113 (1991) 5942.
[22] S. Baer, J.I. Brauman, J. Am. Chem. Soc. 114 (1992) 5733.
[23] L.K. Blair, P.C. Isolani, J. Riveros, J. Am. Chem. Soc. 95 (1973) 1057.
[24] C.R. Moylan, J.A. Dodd, C.-C. Han, J.I. Brauman, J. Chem. Phys. 86 (1987) 5350.
[25] K.F. Lim, J.I. Brauman, J. Chem. Phys. 94 (1991) 7164.
[26] K.F. Lim, R.I. Kier, J. Chem. Phys. 97 (1992) 1072.
[27] R.J. Hinde, G.S. Ezra, Chem. Phys. Lett. 228 (1994) 333.
[28] M.R. Ellenberger, W.E. Farneth, D.A. Dixon, J. Phys. Chem. 85 (1981) 4.
[29] J.J. Grabowski, C.H. DePuy, V.M. Bierbaum, J. Am. Chem. Soc. 105 (1983) 2565.

[30] J.M. Van Doren, S.E. Barlow, C.H. DePuy, V.M. Bierbaum, Int. J. Mass Spectrom. Ion Processes 81 (1987) 85.
[31] T. Su, W.J. Chesnavich, J. Chem. Phys. 76 (1982) 5183.
[32] P.M. Langevin, Ann. Chem. Phys. 5 (1905) 245.
[33] D.B. Milligan, P.F. Wilson, M.J. McEwan, V.G. Anicich, Int. J. Mass Spectrom. 185/186/187 (1999) 663, and references cited therein.
[34] M. Meot-Ner (Mautner), in Gas Phase Ion Chemistry, Vol. 1, M.T. Bowers (Ed.), Academic, New York, 1979, pp. 196–271.
[35] J.T. Yardley, Introduction to Molecular Energy Transfer (Academic, New York, 1980).
[36] P.J. Robinson, K.A. Holbrook, Unimolecular Reactions (Wiley-Interscience, London, 1972).